

Analysis of L5 phase variations in GPS IIF satellites by the raw observation PPP approach



TECHNISCHE
UNIVERSITÄT
DARMSTADT

Sha Liu, Matthias Becker, Florian Reichel

Chair of Physical and Satellite Geodesy, Institute of Geodesy, TU Darmstadt, Germany

1 Introduction

The first GPS IIF satellite was launched in May 2010. Until now (2015 March 1) there are eight Block IIF satellites in service and the remaining four IIF satellites are planned to be launched by 2016. Phase variations are found on the new L5 observations of GPS SVN62 using a linear combination of the three frequencies (Montenbruck, 2010, 2011). In this work, a PPP approach that avoids using any linear combination named raw observation PPP is used to analyze the L5 phase variations for all available GPS IIF satellites. L5 phase variations indicate the unmodelled variations on L5 phase observation residuals. Observation data of 30 IGS MGEX stations with good global distribution, as shown in the Figure 1, are analyzed with this approach.

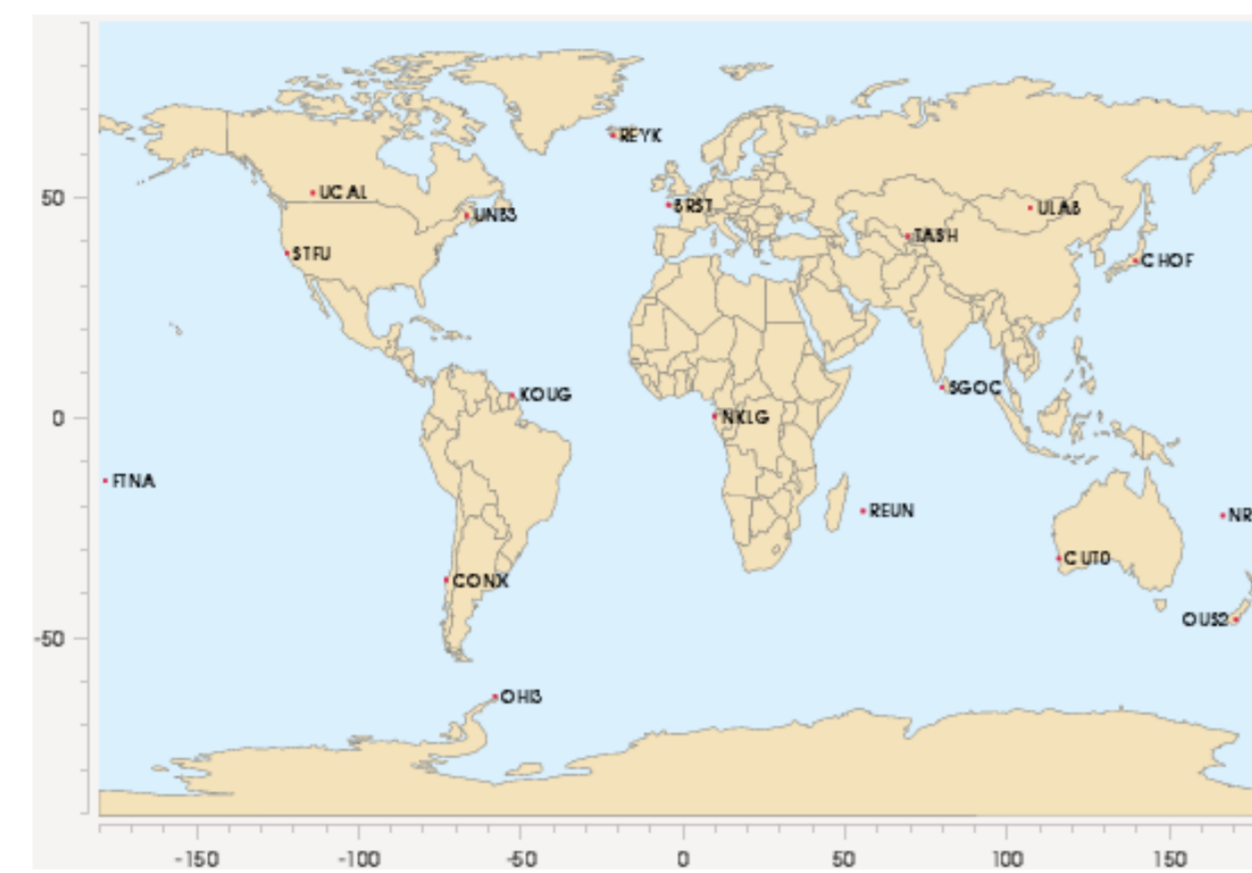


Figure 1: MGEX stations used for the analysis

2 Raw observation PPP approach

The raw observation PPP approach (Schönemann et al. 2011) is an uncombined undifferenced PPP. Compared to the conventional PPP, which builds an ionosphere-free linear combination with the data of 2 frequencies, the raw observation PPP processes the multi-frequency multi-GNSS observations individually and reduces the complexity of modelling in PPP. Epoch-wise STEC values are estimated as unknown parameters together with the station coordinates, receiver clock error, zenith wet delay and UCDs. UCDs are estimated per link, because receiver and satellite UCDs cannot be separated for stand alone PPP.

The observation equations of raw observation PPP valid for all frequencies are:

$$P_i = \rho - c\delta^s + c\delta_r + \delta_{trop} + \delta_{corr} + \frac{40.3}{f_i^2} STEC + UCD_{rec,i} - UCD_{sat,i} + \delta_{MP,P_i} + \epsilon_{P_i}$$

$$L_i = \rho - c\delta^s + c\delta_r + \delta_{trop} + \delta_{corr} - \frac{40.3}{f_i^2} STEC + UPD_{rec,i} - UPD_{sat,i} + \lambda_i N_{f_i} + \delta_{pwi} + \delta_{MP,L_i} + \epsilon_{L_i}$$

P_i, L_i	code and phase observation on frequency i	ρ	the geometry distance
δ^s, δ_r	satellite and receiver clock error	δ_{trop}	the tropospheric delay
δ_{corr}	the corrections are applied in PPP, such as solid earth tides, ocean loading, antenna phase center correction and so on	$STEC$	slant TEC
$UCD_{rec,i}, UCD_{sat,i}$	receiver and satellite uncalibrated code or phase delay on frequency i	δ_{pwi}	phase wind up
$UPD_{rec,i}, UPD_{sat,i}$	receiver and satellite uncalibrated code or phase delay on frequency i	N_{f_i}	carrier phase ambiguity
		$\delta_{MP,P_i}, \delta_{MP,L_i}$	multipath
		$\epsilon_{P_i}, \epsilon_{L_i}$	code and phase observation noise

3 Datasets

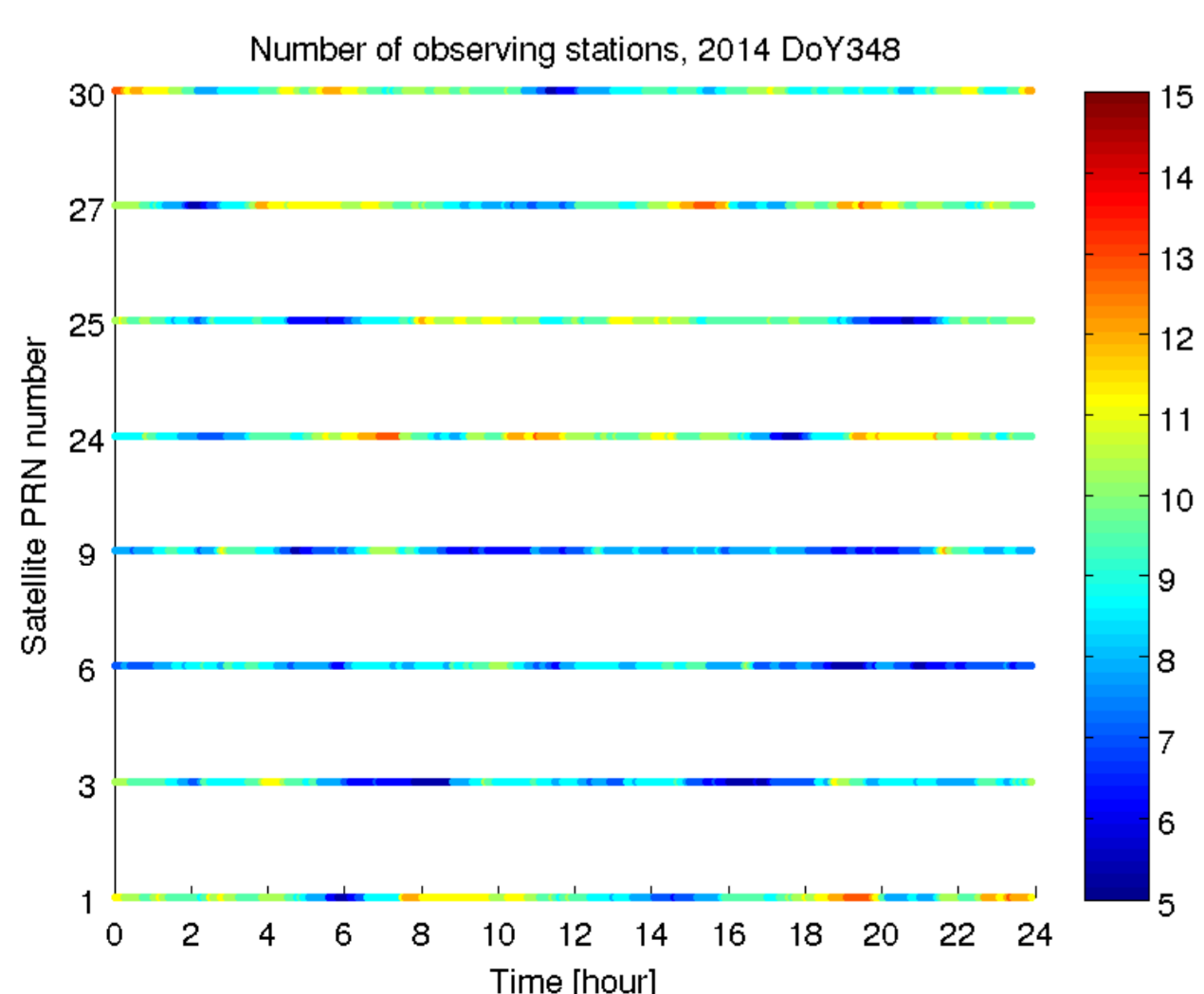


Figure 2: Observability, 2014 DoY 348

Three datasets of the chosen 30 IGS MGEX stations are analyzed. The IGS final products are used for the PPP processing.

- 15 - 21 Jun., 2014 (DoY: 166-172, GPS week: 1797)
- 21 - 27 Sep., 2014 (DoY: 264-270, GPS week: 1811)
- 14 - 20 Dec., 2014 (DoY: 348-354, GPS week: 1823)

Figure 2 illustrates as an example that at least 5 stations can track the GPS satellites simultaneously, the cutoff angle 5 degree is used.

4 Analysis of L5 phase variations

All datasets of the 30 MGEX stations (Figure 1) are analyzed by the raw observation PPP approach. The L5 phase residuals of GPS satellite G27 (SVN66) from all the 30 stations are plotted in Figure 4 as an example. The three subplots show the L5 phase residuals from day of year 166 to 172, 264 to 270 and 348 to 354 respectively. The corresponding sun beta angles of G27 are 13 to 8 degrees, -55 degrees and -9 to -4 degrees.

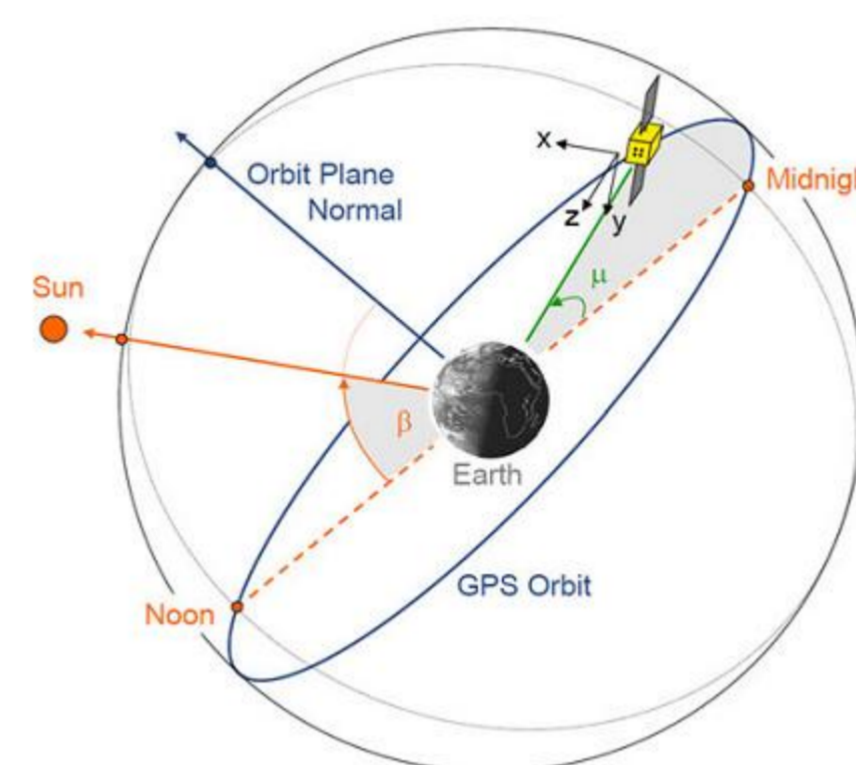


Figure 3: Sun beta angle, (Montenbruck et al., 2011)

It is clear that the amplitude of the L5 residuals is dependent on the sun beta angle, as illustrated in Figure 3. All other GPS Block IIF satellites show a similar behaviour, they are not presented here due to the limited space.

5 Correction of L5 phase variations

The variations of L5 phase residuals can be modelled by a function of the form: (Montenbruck et al., 2011)

$$f = \sum_{i=1}^k A_i \sin(i\mu + \Phi_i)$$

The orbit angle μ (Figure 3) is counted from the midnight line (sun-satellite-earth angle is minimum) to the satellite position. Coefficients A_i and Φ_i are related to the sun beta angle β . Two different sets of coefficients are estimated for low and high sun beta angle.

Two scenarios of the coefficients are applied for raw observation PPP. In scenario 1 (S1), the coefficients are used as derived by Montenbruck (2011) from the difference of the ionosphere-free L1/L2 and L1/L5 phase combination (0.285L1-1.546L2+1.261L5). In scenario 2 (S2), we derived the coefficients from the L5 phase residuals by fitting the above function.

Figure 5 gives the L5 phase residuals of G27 after applying corrections of scenario 1.

	DoY 166-172					DoY 264-270					DoY 348-354				
	β	L1/L2	L5	L5 corr S1	L5 corr S2	β	L1/L2	L5	L5 corr S1	L5 corr S2	β	L1/L2	L5	L5 corr S1	L5 corr S2
G1	60°	3.0	17.0	17.4	8.9	-32°	2.9	13.9	12.2	11.0	-55°	2.9	10.5	9.4	7.9
G3	-	-	-	-	-	-	-	-	-	-	-68°	3.0	7.7	7.4	7.5
G6	60°	2.8	12.5	10.7	9.5	-32°	2.8	14.8	9.8	10.6	-55°	2.9	12.5	10.7	9.5
G9	-	-	-	-	-	53°	2.9	10.9	9.6	10.2	-20°	2.9	21.7	9.8	13.3
G24	-23°	3.0	18.3	11.4	12.9	33°	3.0	14.4	10.4	10.2	20°	3.0	18.5	11.2	13.7
G25	-27°	3.1	27.5	22.6	14.7	-15°	3.0	21.6	7.3	15.3	29°	3.1	16.4	6.8	12.0
G27	10°	3.0	20.4	12.5	10.7	-55°	3.0	12.4	11.6	16.8	-7°	3.0	24.7	14.6	11.5
G30	-25°	2.9	16.1	11.1	9.9	28°	2.9	14.9	10.0	10.4	23°	2.9	17.1	11.2	11.5

Table 1: Sun beta angle and RMS of phase residuals in [mm]

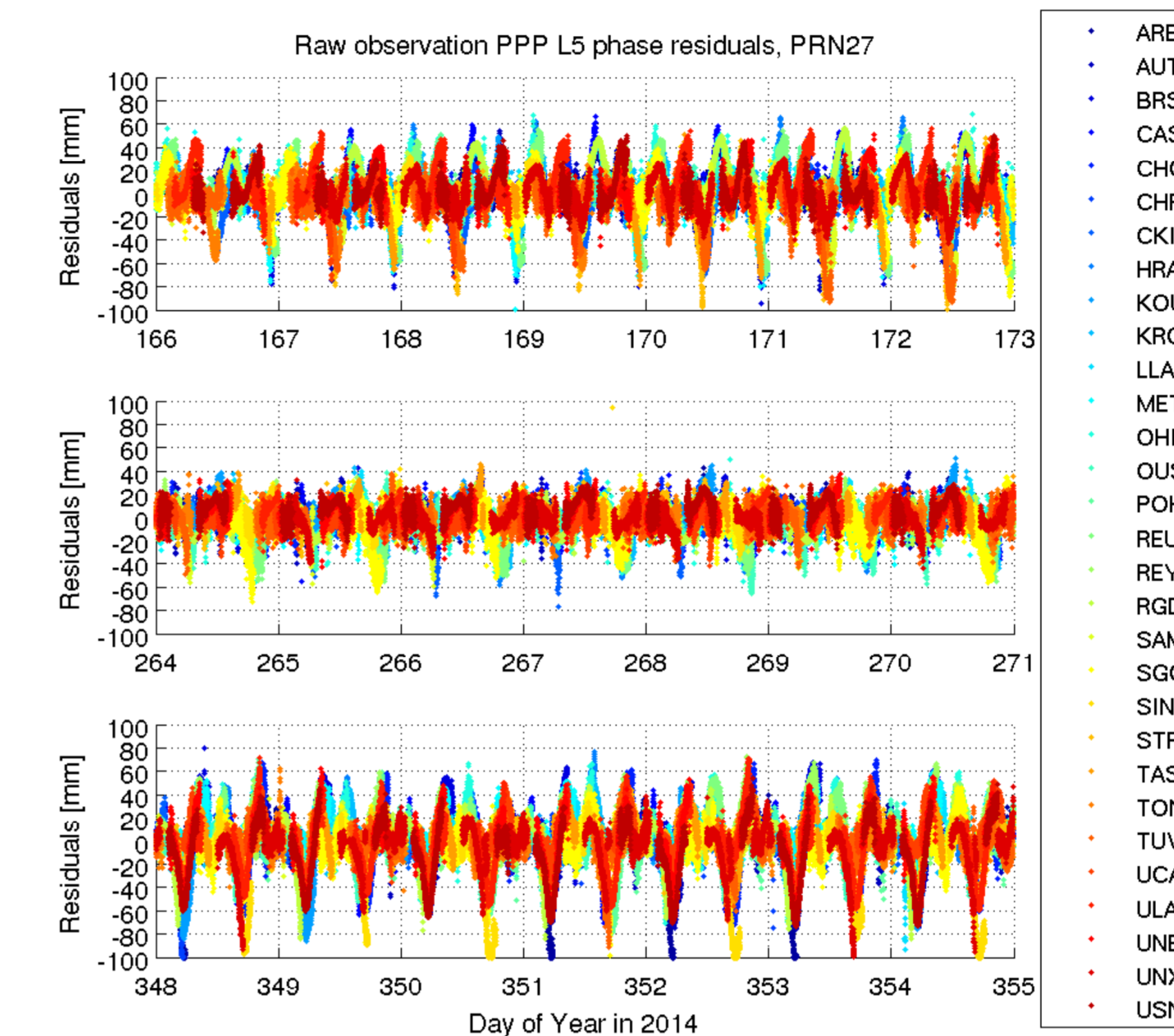


Figure 4: L5 phase residuals of G27

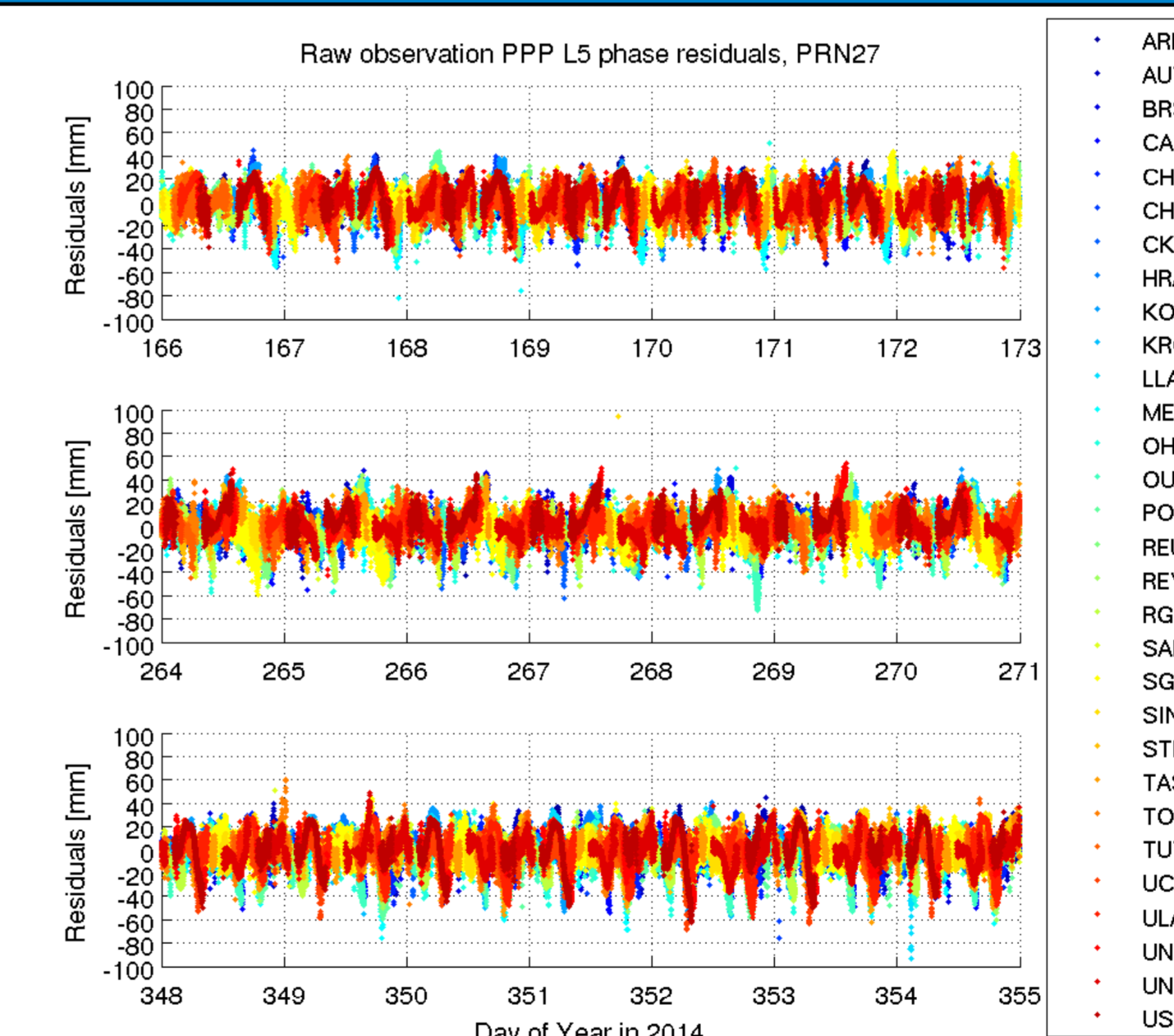


Figure 5: L5 phase residuals of G27 after applying corrections of scenario 1

Table 1 summarizes the sun beta angle, the RMS of the L1, L2 and L5 phase residuals and the L5 phase residuals after applying the corrections of scenario 1 and 2.

The phase variations are significantly reduced by the correction model, especially for the lower sun beta angle case (the top and bottom subplot, Figure 5). Although the coefficients of scenario 1 are derived using the data of SVN62 only, it is seen here that they are suitable for all Block IIF satellites. Satellite specific coefficients of scenario 2 work similarly well. However, the results of the two scenarios can not be compared directly, since the observation period of scenario 2 is much shorter than that of scenario 1. More improvements of scenario 2 are expected by the use of a longer observation period.

6 Conclusion

With the raw observation PPP approach it is possible to analyze the raw observation characteristics without any linear combination. Clear systematic variations on L5 phase residuals are found in all GPS Block IIF satellites. The variations can be corrected with an empirical model. After applying these corrections to the L5 phase observations, the L5 phase variations are significantly diminished.

However, the RMS of L5 phase residuals after correction is still more than 3 times larger as that of L1/L2. Further research should be conducted to seek the reasons of the degraded performance of the L5 phase observations. A significant contribution to the high RMS may be due to the missing L5 antenna phase centre corrections.

Acknowledgement

We thank the Navigation Office at ESA/ESOC for their cooperation. We also thank BKG for the cooperative implementation of the PPP software GEMon and IGS for providing observation data and products.

References

- [Montenbruck, 2010] O. MONTENBRUCK (2010). *The System: Three's the Challenge*. GPS World.
- [Montenbruck et al., 2011] O. MONTENBRUCK, U. HUGENTOBLE, R. DACH, P. STEIGENBERGER and A. HAUSCHILD (2011). *Apparent clock variations of the Block IIF-1 (SVN62) GPS satellite*. GPS Solution.
- [Schönemann et al., 2011] E. SCHÖNEMANN, M. BECKER and T. SPRINGER (2011). *A new Approach for GNSS Analysis in a Multi-GNSS and Multi-Signal Environment*. Journal of Geodetic Science.